Tomas Bata University in Zlín
Faculty of Technology

Doctoral Thesis Summary

Optimalizace zpracování kovových prášků vstřikováním

Powder Injection Molding: Feedstock Tailoring and Process Optimization

Author:	**Ing. Martin Novák, Ph.D.**
Degree programme:	P3909 Process Engineering
Degree course:	3909V013 Tools and Processes
Supervisor:	prof. Ing. Berenika Hausnerová, Ph.D.
External examiners:	prof. Dr. Bernhard Möginger
	prof. Ing. Petr Slobodian, Ph.D.

Zlín, March 2024

©Martin Novák

Published by **Tomas Bata University in Zlín** in the Edition **Doctoral Thesis Summary.**
The publication was issued in the year 2024

Keywords: *highly filled powder compounds, polymer binder, powder injection molding, process optimization*

Klíčová slova: *vysoce plněné práškové směsi, polymerní pojivo, práškové vstřikování, optimalizace procesu*

Full text of the doctoral thesis is available in the Library of TBU in Zlín.

ISBN 978-80-7678-244-0

TABLE OF CONTENTS

ABSTRACT 4
ABSTRAKT 4
THEORETICAL BACKGROUND 5
1. INTRODUCTION 5
2. PIM PROCESS 5
2.1 Issues with the modeling of the feedstock characteristics 6
2.2 Merging of PIM with additive manufacturing 6
3. METHODOLOGY AND PURPOSE OF THE WORK 7
EXPERIMENTAL PART 7
4. MATERIALS AND METHODS 7
4.1 Materials 7
4.1.1 Binder components 7
4.1.2 Powders 8
4.1.3 Additional chemicals 8
4.2 Apparatus 8
5. RESULTS AND DISCUSSION 9
5.1 Feedstock tailoring and preparation 9
5.2 Injection molding of environmentally benign feedstocks 11
5.3 Debinding 12
5.3.1 Solvent debinding 12
5.3.2 Thermal debinding and sintering 12
5.4 Comparison of PIM with ADAM and DMLS 15
5.4.1 Measurements and evaluation of surface properties 18
6. CONCLUSION 21
7. CONTRIBUTIONS TO THE SCIENCE AND PRACTICE 22
BIBLIOGRAPHY 23
LIST OF SYMBOLS AND ABBREVIATIONS 28
LIST OF FIGURES 29
LIST OF TABLES 29
CURRICULUM VITAE 30
LIST OF PUBLICATIONS AND PRESENTATIONS 31

ABSTRACT

Thesis provides a contribution to the development of feedstocks for powder injection molding (PIM). It presents an optimized processing of environmentally benign feedstocks provided on the basis of thorough thermal, morphological, rheological, mechanical, and surface analyses. Specifically, acrawax-based binder was found energy-efficient and eco-friendly for producing stainless steel parts. Comparison of PIM with selected additive manufacturing processing routes can serve as an input for further merging of these techniques.

ABSTRAKT

Tato disertační práce přispívá k vývoji vysoce plněných směsí pro práškové vstřikování (PIM z anglického “powder injection molding”). Reprezentuje optimalizovaný proces environmentálně šetrné směsi vytvořený na základě analýzy termických, morfologických, reologických, mechanických a povrchových vlastností. Polymerní pojivo na bázi acrawaxu bylo shledáno energeticky výhodným a ekologicky šetrným pro výrobu součástek z nerezové oceli. Porovnání PIM s vybranými aditivními způsoby výroby poskytuje podklad pro další prolínání těchto technik.

THEORETICAL BACKGROUND

1. INTRODUCTION

Powder metallurgy is currently used in many industries including the medical, automotive, machinery, electronics, and aerospace, which often require a specific manufacturing process. Powder injection molding (PIM) and additive manufacturing (AM) belong here together with other processes such as die pressing [1], electric current assisted sintering [2], etc.

The quality of the final products depends largely on the chosen processing method [1, 3, 4]. In the case of PIM, the relationship between structure, process, and performance is not fully understood (partly due to a lack of appropriate databases of highly filled compounds).

During PIM, a great number of process variables can result in distortions and (micro)fractures due to residual stresses often caused by non-uniform thermal history. Injection molding machines employed must also guarantee the repeatability of the process, and they should be flexible to process a variety of alloys providing complex-shaped products of required quality [3].

Each PIM feedstock has unique binder composition, powder loading, and powder characteristics such as shape and particle size distribution for which the processing must be optimized [5–7]. This Thesis focuses on the tailoring of environmentally benign feedstocks based on a long-term investigation of the research group at the Centre of Polymer Systems of the TBU in Zlín [6–11] with performance comparable to commercial feedstocks. They contain water-soluble polyethylene glycol (PEG), polyolefin substitutes such as carnauba wax (CW) and acrawax (N, N'- Ethylene Bis-stearamid, AW) [9, 12, 13], and surfactants such as stearic acid (SA). Polylactic acid (PLA) was additionally investigated as a possible substitute for waxes to raise the durability and flexibility of green samples. This would serve a dual purpose, as a prospective goal is to develop "universal" feedstock, which could be utilized in AM as well. Optimized PIM samples were therefore compared to ADAM (atomic diffusion additive manufacturing method) and DMLS (direct metal laser sintering) to identify differences/similarities between both processing routes [13, 14].

2. PIM PROCESS

Generally, the PIM process consists of four basic steps: compounding, injection molding, debinding, and sintering.

First, powder particles are compounded with a suitable binder system into a feedstock and pelletized [15]. Temperature setting can be obtained from differential scanning calorimetry (DSC) and success controlled with scanning electron microscopy (SEM) or energy-dispersive X-ray spectroscopy (EDX) [16].

In the injection molding phase of the PIM process the feedstock, typically thermoplastic, is plasticized and forced into the mold cavity of the desired shape. Here it cools and solidifies. Mold is then opened, and the part (so-called "green") is ejected, the entire process taking usually under a minute [17].

The third step in PIM is debinding. Two or more debinding techniques are commonly combined to accelerate the debinding [17] with solvents e.g., heptane, often utilized first, and thermal debinding later to provide the "brown part" [17].

Sintering is the final step in the PIM process. Here, powder particles fuse together while the sample itself shrinks and densifies. Final mechanical properties vary with different sintering atmospheres, pressures, temperatures, dwell times, etc. [17] Preliminary sintering and thermal debinding curves for testing new materials can be obtained from thermogravimetric (TGA) measurements [18].

2.1 Issues with the modeling of the feedstock characteristics

If PIM conditions are set up improperly, undesirable effects such as the powder/binder separation, the wall-slip effect, flashes, warping after the sintering, and other problems can appear [17]. The viscosity of processed feedstock must be within a certain range [19, 20], shrinkage after processing precisely accounted for [21], powder size, shape [6] and loading [22] must be considered and the type of binder constituents and their molecular weights plays a role too [23]. Additionally, models [20, 24–27] available for polymer melts fit the rheological data of PIM feedstocks only within certain limits. The success of the debinding and sintering steps is evaluated from the mechanical properties of the final samples. These properties can be determined by e.g. tensile test or Vickers microhardness [28–30].

2.2 Merging of PIM with additive manufacturing

The processing of highly filled metal and ceramic feedstocks via PIM and AM has many common features, differing mainly in the method of shaping feedstock into a "green" part. An interesting possibility, is to directly adopt feedstocks developed for PIM in additive manufacturing and merge these two technologies.

Recent trends also point toward "PIM-like" AM technologies e.g., fused deposition modeling (FDM). PIM is advantageous in high-volume production while cheap forming technologies like FDM can provide cheap prototypes before designing an expensive mold for PIM [31]. The PIM feedstocks which are useable in FDM should be flexible and tough so that the filament does not break or is abraded during processing. The viscosity of the melt of this feedstock must be sufficiently low and at the same time not enough for the filament to buckle or slip. Such filaments are currently being tested [32] with first commercial options such as Ultrafuse® 316LX [33] and ADAM method [34] available.

3. METHODOLOGY AND PURPOSE OF THE WORK

Binder systems for PIM are continuously being developed by the PIM research group at the TBU in Zlín. The basis for the development of a novel environmentally benign binder system has been presented in the preceding works [6, 8–12, 16, 23, 35–37] devoted to the molecular interactions of various polymers and waxes together with an investigation of rheological relations between powder characteristics, loading, and binder components.

The goal of this Thesis is to tailor the composition to provide stainless steel feedstocks which are processable and ecological. The supplementary goal is to conduct an investigation into the possibility of modifying them for purposes of AM.

Promising PEG/AW and PEG/CW based feedstocks will be investigated. PEG/PLA based feedstocks will be also considered as they are assumed to provide less brittle feedstock, and thus flexible enough filaments for AM purposes.

The PIM process will be optimized with mechanical properties as the main criterion of success. DSC and TGA data will be utilized to set up mixing, molding, and decomposition temperatures. Rheological properties will be measured on a capillary rheometer to provide the data relevant to the molding step. SEM and EDX techniques will allow the monitoring of aggregates and other processing defects. Mechanical properties in terms of ultimate tensile strength (UTS), elongation at fracture, and yield stress (YS) will be evaluated on the final sintered parts. The results will be compared with the commercially available materials.

Additionally, the mechanical and surface properties of PIM parts will be compared with those processed through DMLS and ADAM. Possible similarities among these techniques will be analyzed with the help of advanced statistical tools.

EXPERIMENTAL PART

4. MATERIALS AND METHODS

4.1 Materials

4.1.1 Binder components

- PEG4000 – Polyethylene glycol with molecular weight 4000 Da, Sinopol, Sino-Japan Chemical Co., Ltd. (Taipei, TW)
- PEG6000 – Polyethylene glycol with molecular weight 6000 Da, Sinopol, Sino-Japan Chemical Co., Ltd. (Taipei, TW)

- AW – Acrawax® C (N,N' Ethylene Bisstearamide), atomized, Lonza (Basel, CH)
- CW – Carnauba wax (2442), Kahl GmbH & Co. KG (Trittau, DE).
- PW – Paraffin wax, paraffinum solidum (FAGRON, Olomouc, CZ)
- PLA – Polylactic acid, Ingeo 4043D, NatureWorks LLC (Plymouth, USA)
- SA – Stearic acid, P-LAB a.s. (Prague, CZ)

4.1.2 Powders

- 17-4PH (PIM_{DMLS}) – D_{50} = 31.4 μm, 7.8 g/cm^3, Carpenter Additive (Widnes, GB)
- 17-4PH (PIM_{PIM}) – D_{50} = 8 μm, 7.8 g/cm^3, Sandvik Osprey (Sandviken, SE)
- 316L – D_{50} = 8 μm, 7.99 g/cm^3, Sandvik Osprey (Sandviken, SE)
- ADAM – Metal X 17-4PH feedstock (Markforged, Watertown, USA), powder composition itself was undisclosed

4.1.3 Additional chemicals

Water with added 2 vol% corrosion inhibitor - Inhibitor 4000 (Zschimmer & Schwarz GmbH & Co KG, Lahnstein, DE) - for debinding of PIM samples.

Markforged WASH-1 (Markforged, Watertown, USA) - for debinding of ADAM samples.

An aqueous solution of HCl + HNO_3 + $FeCl_3$ was employed to uncover grain boundaries for the purpose of microstructure observation.

4.2 Apparatus

Compounding was performed with the help of:

- Twin-screw extruder - Scientific Twin Screw Extruder (Labtech, California, USA) and Brabender Plasti-Corder PL 2000 (Brabender GmbH & Co. KG, Duisburg, DE)
- Internal mixer - Brabender Plastograph, (Brabender GmbH &Co, KG, Duisburg, DE) and MZ05, Winkworth (Winkworth Machinery Ltd, Basingstoke, GB)

Injection molding was done using a PIM injection molding machine – Allrounder 370S 700-100, Arburg (ARBURG GmbH + Co KG, Lössburg, DE).

Additive manufacturing techniques used:

- DMLS machine - EOS M290 (EOS GmbH, Krailling, DE) was used for the preparation of DMLS samples
- ADAM machine - Metal X system (Markforged, Watertown, USA) was used for the preparation of 3D printed and sintered samples

Sintering furnace MIM 3016 (CLASIC CZ s.r.o., Revnice, CZ) was used for the thermal debinding and sintering.

Testing equipment:

- Thermogravimetric analyzer TGA Q50 (TA Instruments, New Castle, USA)
- Differential scanning calorimeter DSC1 Mettler Toledo (Mettler Toledo, Columbus, USA)
- Capillary rheometer Göettfert 50 (GÖTTFERT Werkstoff-Prüfmaschinen GmbH, Buchen, DE)
- Scanning electron microscope Phenom Pro (Thermo Fisher Scientific, Phenom-World B.V., Eindhoven, NL); SEM/EDX microscope VEGA II LMU (Tescan Ltd., CZ) and metallographic microscope (Olympus GX5, Olympus IMS, Tokyo, JP) were utilized
- Laser Diffraction Particle Size Analyzer Malvern Mastersizer 3000 (Malvern Panalytical Ltd, Malvern, GB)
- Variety of laboratory scales
- Tensile testing machine ZWICK Materialprüfung 1456 (ZwickRoell GmbH & Co.KG, Ulm, DE) was used to evaluate elongation at fracture, UTS, and YS according to ASTM standard method E8M-00
- Micro-Combi Tester instrument (CSM Instruments SA, Peseux, CH)
- 3D scanner TALYSURF CLI 500 (Taylor Hobson, Leicester, GB)

Utilized statistics were the method of principal components and a type of cluster analysis - Ward method.

5. RESULTS AND DISCUSSION

5.1 Feedstock tailoring and preparation

Development of PIM feedstocks seeks: efficient processability and/or lesser ecological impact of the manufacturing process, no powder/binder separation, low sensitivity to temperature, easy and fast debinding without defects, low contaminants in the brown sample, and overall to surpass commercial available materials in processability and mechanical properties.

Particle size distribution was measured. Obtained D_{50} of powders was close to those declared, specifically 31.8, 8.2 and 8.5 μm for PIM_{DMLS}, PIM_{PIM}, and 316L respectively.

During feedstock preparation, as a first step, a binder mix was prepared. Components in predetermined ratios (59 wt% PEG, 28 wt% AW or CW or PLA, 12 wt% PW, and 1 wt% SA) were compounded and then extruded. PEG in this work is a compound with a 1:1 ratio of PEG4000 and PEG6000. Twelve other compositions containing PLA were also tested, from which only 59/28/12/1 wt% PEG/AW/PLA/SA composition at 55 vol% loading was utilized further for molding and debinding tests. The initial heating profile for AW and CW-based binder was too high when using values from DSC, the same after adding the powder to create feedstock, resulting in too low viscosity to prevent flow instabilities. The values of CW and AW melting points from the literature were confirmed through DSC, with AW-binder peaking at ~137 °C, and CW at ~81 °C. Optimized profiles are [13, 14]:

- AW binder = 65/60/60/55/50/45 °C, 100 RPM.
    a. AW-316L feedstock = 60 vol%, 65/60/55 °C, 20 RPM, addendum: temperature of middle zone rose by 15 °C during processing by friction.
    b. AW-PIM_{PIM} feedstock = 60 vol%, 65/60/55 °C, 20 RPM, z-blade mixing 15 min, 80 °C, 20-25 RPM.
    c. AW-PIM_{DMLS} feedstock = 90/75/70 °C, 20 RPM, z-blade mixing 15 min, 80 °C, 20-25 RPM.
- CW binder = 55/58/45 °C, 60 RPM.
    a. CW-316L feedstock = 60 vol%, 60/60/50 °C, 20 RPM
- PLA binder = PEG/AW/PLA/SA mix containing 0-28 wt% of AW, 12-87 wt% PLA, 12-59 wt% PEG and 1 % SA. An additional mix of 59/28/12/1 wt% PEG/PLA/PW/SA was also tested.
    a. PLA feedstock = 60 vol%, z-blade mixing 5 min per batch, 170 °C, 30 RPM, 55 vol% (59/28/12/1 wt% PEG/AW/PLA/SA) and 60 vol% (59/28/12/1 wt% PEG/PLA/PW/SA) powder loading.

It was found necessary to add only ~3/4 of powder during the first cycle of compounding and rest in the second run to prevent seizing up of the extruder. All feedstocks were therefore extruded twice, and their homogeneity was controlled by SEM. PIM_{PIM} and PIM_{DMLS} feedstocks (17-4PH steel) were additionally mixed once more in a Z-blade mixer to observe possible differences in homogeneity. No significant differences were observed.

5.2 Injection molding of environmentally benign feedstocks

The molding temperatures tested for the particular heating zones of AW-based feedstock are depicted in Table 1 and based on the melting point of last-to-melt component and rheometric measurements (apparent shear rate $\dot{\gamma}_a$=10-4000 s^{-1}, 20/0.5 capillary). Four tests were performed for CW-316L starting with 80/120/90/80/75/30 °C temperature profile. At higher temperatures viscosity of feedstock was again too low to be properly molded, leading to flow instabilities. Similar instabilities can be also observed when the temperature is too low. An example can be seen in Figure 1.

Table 1 Setup of conditions for injection molding of Acrawax (AW) feedstock

Temperature [°C]	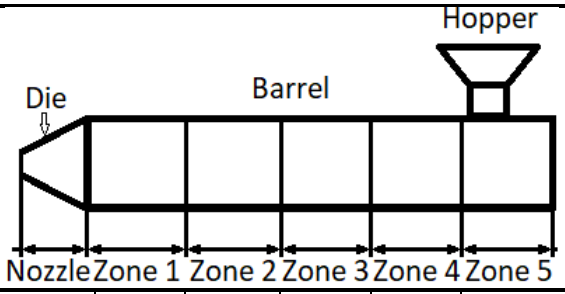					**Satisfactory**
Test 1	110	150	130	90	85	50	No
Test 2	90	130	110	80	75	40	No
Test 3	80	120	90	80	75	30	No
Test 4	75	110	90	80	75	30	No
Test 5	75	95	85	80	75	30	Yes
Test 6	75	70	70	60	45	35	Partly

Test 6 in Table 1 was only partially satisfactory as problems appeared after sintering, likely due to cracks and inner voids.

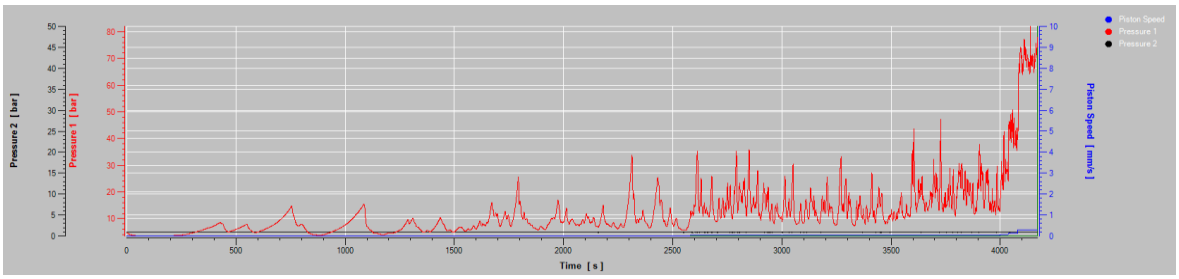

Figure 1 Flow instabilities during rheological measurements of CW-based feedstock at 70 °C

The optimum setup for AW included a 75/95/85/80/75/20 °C heating profile, screw stroke of 60 mm, cooling time of 30 s, injection pressure of 1000 bar, first hold pressure 800 bar for 5 s and second hold pressure of 150 bar for 2 s. Both PIM_{PIM} and PIM_{DMLS} had identical molding setups and provided samples without obvious defects. The optimum profile for CW-316L was 65/70/90/80/60/30 °C h,

screw stroke 70 mm, cooling time 10 s, injection pressure 500 bar, first hold pressure 400 bar for 5 s, and second hold pressure of 50 bar for 0.5 s together with the rest of the used molding parameters. Molding and compounding conditions for the CW- and PLA-based feedstock were not fully optimized according to mechanical properties due to problems during solvent debinding, but samples were visually pristine. Profile of PLA feedstocks was 160/180/175/165/140/30 °C, screw stroke 70 mm, cooling time 30 s, injection pressure 1000 bar, first hold pressure 800 bar for 5 s and second hold pressure of 150 bar for 2 s.

5.3 Debinding

5.3.1 Solvent debinding

Preliminary debinding tests (water, ≤50 °C) were conducted on all three prepared types (AW, CW, PLA) of feedstocks to see if the processing is possible before preparing larger batches. CW- and PLA-based feedstocks appeared to be unsuitable for water debinding due to cracking, blistering, delamination, and even full dissolution of the PLA sample.

The AW-based feedstock also exhibited signs of erosion after 8 h, but 7 h of debinding time led to the relative loss of the mass of 4.0±0.1 wt% (80.5 wt% of PEG) without observable problems. The 6-7 h debinding time was therefore chosen as optimal for AW feedstock [13].

5.3.2 Thermal debinding and sintering

The thermal debinding program for AW- (Figure 2) and CW-based feedstocks was first set based on the results from the TGA. In the case of AW, the debinding and sintering would proceed with a combination of water and thermal debinding, while due to the failure of water debinding for CW-based feedstock, an attempt to debind them fully thermally was made. Nitrogen atmosphere was used for both TGA testing and following sintering. According to previous studies, it also provides the highest strength to the sample but leaves it brittle with a ductility of about 15 % for 316L steel [13, 38]. This inert atmosphere was used (balance 40 ml/min; sample 60 ml/min) to simulate conditions of thermal debinding from 30 to 700 °C with a speed of 5 °C/min [13].

The AW-based feedstock was designed with step-by-step thermal debinding in mind. As can be seen in Figure 2 below, this intent was realized, resulting in gradual loss of weight and overall gentle thermal debinding due to preexisting porous structure inside samples as a result of water debinding.

TGA of CW-based feedstock (316L steel powder), showed only two distinguishable weight loss steps with the second one representing a weight loss of 3.37 wt%. As CW feedstock could not be debound in water without cracking, thermally debinding based on TGA was attempted using a nitrogen atmosphere.

This failed as the sample was partially burned, warped, and melted. Full focus was therefore given to AW-based binder.

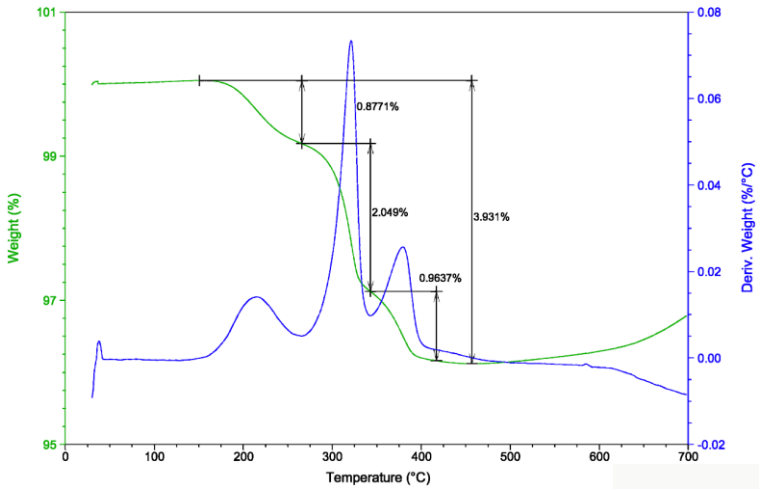

Figure 2 Thermogravimetric analysis of AW-based feedstock with 316L powder after water debinding [13]

Testing specimens were type A according to EN ISO 2740:2009(E). The crosshead speed was 0.7 mm/min. The mechanical properties of the final samples are affected by the sintering program. Variances in temperature, ramp, and dwell time all lead to different results. Higher temperatures, for example, may lead to the formation of larger grain structures leading to worse mechanical properties [13, 17]. The AW-based samples containing 316L steel were debound and sintered at various conditions. The influence of the sintering speed (ramp) of 5, 10, and 15 °C in the temperature range from 450 to 1360 °C, on the mechanical properties of the samples was investigated. The optimized profile included starting from rest temperature to 250 °C with 3 °C/min ramp, hold for 60 min followed by 2 °C/min ramp to 450 °C, hold 20 min and final ramp to 1360 °C where sintering lasted for 150 min [13].

Interestingly, nitrogen atmosphere could not be used for 17-4PH steel, as samples showed low density and golden brown discoloration. The low density of samples sintered in nitrogen-containing atmospheres when compared with pure hydrogen was noted in the literature [17].

Differences in mechanical properties resulting from sintering speeds of 5, 10, and 15 °C/min can be seen in Table 2. Vickers (*Hv*) microhardness of 316L was tested on three samples, each at 4 different places for each investigated speed (5, 10, and 15 °C/min). The gauge length used was 40 mm. These differences may be explained through variance in structure and by the presence of microscopic defects induced during debinding and sintering. Microstructure analysis of

carefully polished and etched sintered samples was therefore performed on a metallographic microscope [13].

At the slow speed of 5 °C/min, relatively small but numerous pores could be observed with the formation of the largest grains (90±35) μm. The microstructure, in this case, was austenitic with only rare deformation twins, and even deformation-induced martensite. Sintered density was the highest of the three compared [13].

Table 2 Mechanical properties of sintered 316L samples (modified from [13])

Mechanical Property	**Speed [°C/min]**		
	5	**10**	**15**
UTS [MPa]	557±34	535±45	546±41
YS [MPa]	264±6	267±5	264±2
Elongation at fracture [%]	31±8	26±11	28±9
Sintered density [g/cm^3]	7.27	7.16	7.22
Vickers Microhardness [H_v]	150±6	145±7	145±11

When the sintering speed was raised to 10 °C/min, the number of defects increased (Figure 3a) explaining lower mechanical properties and greater standard deviation of this series. The grain size was (53±25) μm and sintered density lowest. The heating rate of 15 °C/min resulted in the structure with (62±29) μm grains. The presence of defects, such as vortexes located around larger pores, has been confirmed for this sintering profile as shown in Figure 3b. Deformation-induced martensite is in this case located mainly in the vicinity of the vortexes and the borders of the defects [13]. This is similar to the results of Omar and Subuki [39] where 5 °C/min samples showed small, regularly shaped pores, while 15 °C/min samples tended to have a combination of small quasi-spherical pores with larger and irregular pores. In this case, however, 10 °C/min samples provided samples with the lowest porosity, reaching up to 98 % sintered density when compared to 97 % of 5 and 15 °C/min. High porosity at fast heating rates occurs as pores tend to get isolated inside grains where they cannot be eliminated [17, 39].

Smaller grains usually mean larger UTS and YS, while bigger pores lead to the contrary [40]. The amount of induced martensite may also affect mechanical properties. The 5 °C/min speed was therefore considered the best option [13].

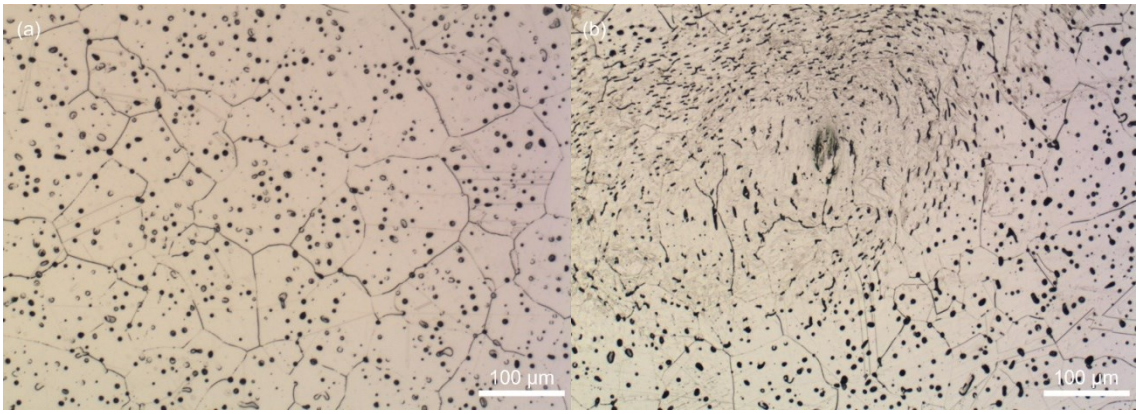

Figure 3 Microstructure of 316L steel sintered at: (a) 5 °C/min; (b) 15 °C/min [13]

5.4 Comparison of PIM with ADAM and DMLS

To meet the current trend of merging PIM with AM, both approaches should result in products of similar quality. However, for both technologies, there are still inherent compromises in the compositions of the materials, product design, process parameters, and resulting properties, such as sintered density, residual stresses, and mechanical integrity [4, 14, 41].

In this thesis, we have chosen to investigate the PIM processability of both fine 17-4PH powder (PIM_{PIM}), and coarser 17-4 PH powder formulated originally for DMLS (PIM_{DMLS}). Their tensile and yield strengths as well as the elongation at fracture are determined and compared to those produced using atomic diffusion additive manufacturing (ADAM) and direct metal laser sintering (DMLS). Surface properties are evaluated through a 3D scanner and analyzed with advanced statistical tools [14].

5.4.1 Production of testing samples

Rheological data were determined using a capillary rheometer on capillaries with 20/1 and 20/0.5 length-to-diameter ratios. The $\dot{\gamma}_a$ range was 35 - 4000 s^{-1}. These measurements (Figure 4) agree with the previously observed complex dilatant/pseudoplastic behavior of PIM feedstocks [14, 37, 42]. The change from pseudoplastic to dilatant flow and back was explained in [20].

As can be seen, the feedstock containing larger particles (PIM_{DMLS}) exhibits higher viscosity than based on fine particles (PIM_{PIM}), which is consistent with the previous findings of Mukund *et* al. [10]. The pseudoplastic character of the flow observed at higher $\dot{\gamma}_a$ (approx. 300 s^{-1}) for PIM_{DMLS} and PIM_{PIM} (Figure 4) is desirable for processing.

Powder/binder separation was observed during the measurement of PIM_{DMLS} with 20/0.5 mm capillary, with an accumulation of powder on the walls. However, this led to no observable issues in production, likely due to the larger size of

nozzles used (2.5 and 3 mm). Capillary 20/1 was also tested, however, significant pressure instabilities at higher $\dot{\gamma}_a$ led to unreliable values [14].

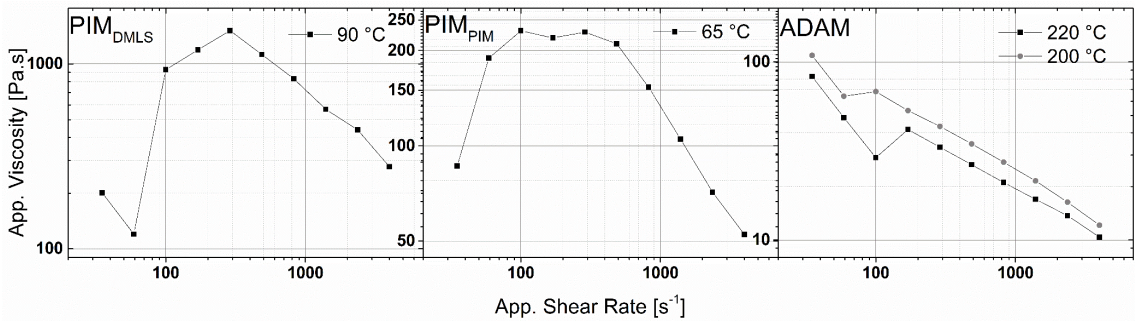

Figure 4 Rheological measurements of utilized feedstocks (modified from [14]*)*

ADAM filament degraded during rheological tests at 220 °C (see Figure 4) as evidenced by evolving gas. This was a temperature provided by the filament supplier. The second measurement at a 20 °C lower temperature was therefore provided [14].

Optimization was done with the same temperature setup (Tests 1 to 5) as in the case of AW-feedstock (Table 1). Higher injection pressures (up to 1300 bar) were also considered in the case of PIM_{DMLS}, however, the identical 1000 bar molding pressure as for PIM_{PIM} and AW-316L feedstock appeared optimal without flashing and short shots. The infill of ADAM was 100 % using a +45°/-45° infill angle. The layer thickness was 0.15 mm and the nozzle diameter was 0.4 mm. Debinding of both PIM_{PIM} and PIM_{DMLS} was done at first with the same setup as in the case of AW-316L feedstock (50 °C water bath, 2 vol% corrosion inhibitor). Retesting was done for 6-10 h debinding times due to blistering after sintering of some samples, however without the desired effect. ADAM samples utilized the Wash-1 debinding system from Markforged [14].

The initial sintering program set-up for 17-4PH steel powders started at rest temperature with a ramp of 3 °C/min to 250 °C and 60 min hold; followed by 2 °C/min heating to 450 °C and 20 min hold. Final heating was at the rate of 5 °C/min up to 1300 °C as the final temperature where the sample was sintered for 3 h followed by free cooling till 90 °C. Nitrogen as an atmosphere was tested first, however, densification of PIM_{DMLS} samples was poor, and thus it was substituted with hydrogen. This program was then further refined as the results of mechanical tests have proven to be poor when used for 17-4PH steel, though the final temperature stayed the same (1300 °C). First hold temperature had to be lowered to 200 °C and hold time at 450 °C extended to 60 min from the original 20 min. Change in thermal debinding and sintering atmosphere for 17-4PH steel to hydrogen resulted in greater relative densities after sintering (up to ~14 % shrinkage after sintering) [14].

Laser sintered samples of 17-4PH powder were designated as DMLS in case of untreated surface and as $DMLS_{Blasted}$ when samples were surface treated through sandblasting. Samples were printed laying flat in the powder bed to achieve high UTS, their layer thickness was 0.05 mm [14].

5.4.2 Mechanical performance

Optimization of the sintering programs of the samples was done on the basis of these mechanical performances, Table 3. A 30 mm gauge length was utilized for this series. Optimization tended to lower standard deviation while average values themselves rose significantly. After optimization, the standard deviation for UTS and YS of $PIM_{PIM}3$ approached values of DMLS.

Ductility (elongation at fracture) of the optimized "$PIM_{PIM}3$" sample, exhibits a high standard deviation - several times larger than $PIM_{DMLS}2$. This may be due to microfractures or chemical changes during the thermal debinding segment of the process with the latter more likely. PIM_{DMLS} samples did not experience blistering and cracking, likely due to larger pore channels as it is known that coarser powders can be debound faster [14, 17, 43]. Particle size distribution of $PIM_{PIM}3$, loading, and binder composition also remained the same as previous AW-based feedstock with 316L steel and was therefore discarded as an explanation.

Table 3 Mechanical properties of sintered samples made from 17-4PH steel (modified from [14])

Method	UTS [MPa]	YS [MPa]	Elongation at fracture [%]
DMLS	1140±15	510±17	19±0.9
$DMLS_{Blasted}$	1140±6.7	510±11	18±2.2
$PIM_{DMLS}1$	600±41	510±39	1.8±0.8
$PIM_{DMLS}2$	750±47	640±56	2.1±0.3
$PIM_{PIM}1$	680±100	-	0.6±0.1
$PIM_{PIM}2$	870±63	780±23	1.5±0.7
$PIM_{PIM}3$	980±14	800±14	3.3±1.6
ADAM	880±8.0	730±11	4.5±0.3

The second assumption was the influence of the sintering atmosphere on the speed of gas development. The catalytic effect of powders on debinding was noted in the works of Aggarwal *et* al. [44] and Lin *et* al. [45]. This was tested later on with EDX (Table 4). An intermediate step with thermal debinding in a nitrogen atmosphere was used and results were observed. Even the best-performing program did not provide pristine testing samples if they contained large flat

surfaces. Gaseous products were likely entrapped by a thin outer low-permeability layer that is created during debinding. It is unlikely that this layer was created during the water debinding phase but may be in fact a thin film of liquid that appears during thermal debinding. Large amounts of carbon left in burned samples could be observed together with some small differences in ratios of elements such as nickel and copper and mainly between iron and chromium in the alloy (Table 4). This lends credibility to the catalytic effect hypothesis.

Further refinement of the PIM process for 17-4PH steel in AW feedstock is needed and will be a subject of the following research together with the effects of the atmosphere on the chemical structure of steel powders. However, defects appeared only on a surface level and were absent from the stem of the tensile specimens, therefore likely not affecting mechanical properties.

Attempts were also made to process AW-based feedstock with 316L by Arburg plastic freeforming, but these led to flow instabilities during printing and significant wear of the nozzle. However, the results obtained with finer zirconia powder were promising. Therefore, the finer steel powders should be the subject of further study.

Table 4 EDX analysis of burned and unburnt samples of 17-4PH steel feedstock debound in a nitrogen atmosphere

Element	Burned sample		Unburnt sample	
	Weight%	Atomic%	Weight%	Atomic%
C K	28.18	64.34	8.19	29.07
Si K	0.31	0.30	0.42	0.64
Cr K	12.04	6.35	17.23	14.13
Fe K	54.78	26.90	67.40	51.44
Ni K	2.29	1.07	3.41	2.47
Cu K	2.39	1.03	3.34	2.24

5.4.1 Measurements and evaluation of surface properties

A contactless 3D scanner was used for the surface analysis of the sintered parts produced via PIM, ADAM, and DMLS, sampling rate was 20 Hz, maximum interface measurement mode, 4×4 mm measured area (according to ISO 4288) with 25 μm spacing and 161 traces for each measurement [14]. Due to artifacts on the surface, only the least affected sides were evaluated. Waviness, and its effect on values, was for calculations removed utilizing the Fast Furrier transformation, it is still however present in the graphs showing the 3D surface maps [14].

As can be seen in Table 5, PIM_{PIM} was smoothest, with the lowest *Ra* and *Rz* from the investigated samples. Sandblasting after DMLS ($DMLS_{Blasted}$ samples did not create a better surface than PIM_{PIM} but it reduced the standard deviation of *Ra* of DMLS samples from 0.32 μm to 0.18 μm. In both parameters, the DMLS provided a worse surface than PIM utilizing finer powders (PIM_{PIM}) [14].

Table 5 Surface parameters of DMLS, ADAM, and PIM samples [14]

Method	***Ra* [μm]**	***Rz* [μm]**	***RSm* [μm]**	***Rz/RSm***	***Rz/Ra***
PIM_{DMLS}	2.44±0.19	14.08±1.40	17.99±1.16	0.78	5.77
PIM_{PIM}	1.73±0.11	9.68±0.98	16.75±0.97	0.58	5.61
DMLS	2.06±0.32	10.97±1.86	22.93±2.53	0.48	5.31
$DMLS_{Blasted}$	1.98±0.18	10.32±1.10	21.70±1.47	0.48	5.20
ADAM	3.04±0.18	16.67±1.34	24.26±1.58	0.69	5.49

The *RSm* parameter shows the frequency of amplitudes - how often the dip in the surface is detected. ADAM had the highest *RSm* parameter, and DMLS samples less so. *RSm* of PIM_{DMLS} was not as high as expected for such large particles, being only 18 μm (showing a relatively high frequency of dips) compared to the average size of PIM_{DMLS} particles of 31.4 μm. A possible explanation is a greater representation of smaller particles on the surface, likely forced there by pressure during injection molding to fill in gaps between larger particles and the surface [14].

Greater *RSm* values in DMLS samples indicate a greater degree of fusion in comparison to PIM_{DMLS}. As DMLS is a laser sintering method, it fuses particles as they melt, while sintering depends on the gradual development of sintering bonds. Dips on the surface are therefore less likely to be detected in the case of DMLS. This is reflected in the higher *Rz/RSm* ratio with a possible correlation between this ratio and ductility (DMLS samples were more ductile) [14].

The *Ra* parameter has been chosen for comparison of surface similarities due to its common use. Two of the available methods were utilized for this purpose. Namely the method of principal components (PCA) and cluster analysis (CA) – specifically Ward's method. PCA method suggested that a similarity apparently exists between PIM_{DMLS} and DMLS methods with their negative first component of roughness vectors. On the other hand, ADAM, PIM_{PIM}, and $DMLS_{Blasted}$ all differ from them, as their first component is positive. If the second component was considered too, the loading plot would be divided into four quadrants, with only ADAM and PIM_{PIM} sharing the same quadrant [14].

The highest similarity level was found between PIM_{PIM} and ADAM - approximately 58 % according to CA. Between DMLS and PIM_{DMLS} it reached

53 %, while $DMLS_{Blasted}$ was similar to PIM_{PIM} and ADAM at approximately 45 %. The similarity between the two cluster groups (PIM_{PIM}, ADAM, and $DMLS_{Blasted}$ versus PIM_{DMLS} and DMLS) is only 32 % and considered unrelated [14].

While PIM and ADAM are considered most similar by CA, their average values of *Ra* differ significantly. This shows that utilized methods do not consider only absolute values of means, but artifacts left by processing may play a role too. Additionally, due to its high average *Ra* values, the ADAM surface cannot be treated as one which does not need surface treatment postprocessing [14].

The rough surface of ADAM samples suggests the use of larger-size particles, however, according to SEM/EDX observations, the ADAM samples contained only 0.4 to 8 μm particles. Temperature and final dwell time were kept the same. Roughness is additionally affected by the feedstock composition and process parameters used [46]. This work shows that the surface provided by each processing method (Figure 5) is unique, discernible even by the naked eye with their specific artifacts affecting the results, and likely being the main contributor to surface properties [14].

Some artifacts left behind by DMLS were even so severe, that some datapoints were excluded automatically by the program from a dataset. However, it cannot be considered to be an error, as it is an inbuilt function of the equipment to prevent results from being skewed by outliers. These pits might be a result of a split-second too-long dwell of laser on a particular spot, remnant pores in the structure, or simply overall overheating of a surface resulting in pitting, and possibly could be eliminated by further optimization of the process. Sandblasting appeared to smooth them down too, as they were not so visible on $DMLS_{Blasted}$ samples [14].

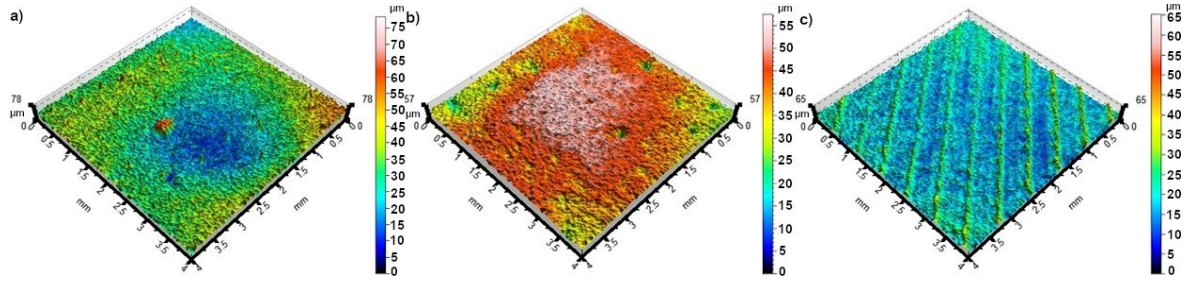

Figure 5 3D surface maps of: a) PIM_{PIM}; b) DMLS; c) ADAM [14]

Additionally, the powder loading is one of the relevant factors too. As it was not provided for ADAM feedstock, it had to be calculated. Therefore, the sintered density was measured through the Archimedes method, and then the powder loading was calculated from relative density and shrinkage. Calculated powder

loading in ADAM is ~60.5 vol%. This is very similar to the loading used for PIM feedstock. Thus, the effect of the loading might be excluded too [14].

The influence of mold surface was not evaluated in this work. It is a legitimate concern, but the possibility of mold defects transfer is limited due to relatively large size of powder particles used.

To summarize, based on subjective evaluations from observation of resulting 3D maps and observation of the sample itself, the processing method plays the greatest role in the resulting sintered surface characteristics.

6. CONCLUSION

In this Thesis, it has been shown that a recently developed acrawax/paraffin wax/polyethylene glycol (AW/PW/PEG)-based binder is processable under lower compounding and molding temperatures than commercially available systems. Due to the PEG component, this feedstock can be partly debound in water. Paraffin wax and stearic acid lowered the viscosity of the feedstocks, while AW acted as a backbone having good adhesion to powder as well as other binder components.

The resulting 316L feedstocks provided samples with mechanical properties comparable to those of commercial feedstock PolyMIM® 316L. Their elongation was approx. 30 % when compared to 40 % provided by commercial feedstock, while their tensile strength (UTS = 557±34 MPa) and yield strength (YS = 264±6 MPa) were higher than that of PolyMIM® 316L (UTS ≥ 450 MPa; YS ≥ 140 MPa) [47]. Thus, the resulting stainless steel feedstocks represent more ecological and economical solution due to low processing temperatures and benign solvents and atmospheres useable during debinding and sintering.

The surface parameters were investigated for injection molded (PIM) 17-4PH feedstocks with fine (PIM_{PIM} designation) and coarse (PIM_{DMLS}) powders, laser sintered samples with ($DMLS_{Blasted}$) and without (DMLS) surface treatment, and for those made through material extrusion method (ADAM). This investigation was performed to ascertain similarity between PIM and additive manufacturing methods as high degree of similarity between surfaces would be desirable in practice due to complementarity of both methods.

The surface parameters of samples differed significantly depending on the method chosen. However, rather unexpectedly high degree of similarity, calculated by Ward's method, between PIM_{PIM} and ADAM samples was observed. It seems that without processing artifacts, ADAM and PIM_{PIM} are somewhat similar, which is reflected also by their similar relative densities of 94.0 and 92.7 %, respectively [14]. The best surface overall, according to surface roughness measurements, was achieved in the case of PIM_{PIM} with *Ra* of 1.73±0.11 μm and *Rz* of 9.68±0.98 μm. DMLS samples were also acceptable, with

sandblasting having only a small effect on the values, but with a larger effect on their standard deviation with *Ra* of 2.06±0.32 μm without surface treatment and 1.98±0.18 μm with sandblasting. PIM_{DMLS} samples had *Ra* of 2.44±0.19 μm and *Rz* of 14.08±1.40 μm, while ADAM samples were worst in terms of *Ra* and *Rz* with *Ra* of 3.04±0.18 μm and *Rz* of 16.67±1.34 μm. Results from tensile tests also prove that PIM parts may successfully compete with DMLS samples, which showed the highest tensile strength (1140±15 MPa) and elongation at fracture (19±0.9 %), its yield strength was lower (510±17 MPa). For comparison, the UTS of PIM_{PIM} was 980±14 MPa, YS 800±14 MPa, and elongation 3.3±1.6 %. Overall, it may be concluded that AM techniques in terms of main quality parameters such as surface finish are still far from those reached with PIM [14].

7. CONTRIBUTIONS TO THE SCIENCE AND PRACTICE

Considering the still increasing proliferation of additive manufacturing methods, their combination with the large-scale production capabilities of PIM is beneficial for industrial practice, especially if there are also ecological advantages.

The benefits of this work can be summarized in the following points:

1) The binder system based on Acrawax and PEG as main components is processed at substantially low processing temperatures. It is partially debound in water without the necessity to employ chemical solvents. A cheaper nitrogen atmosphere is useable for the sintering of 316L stainless steel feedstocks.
2) Due to the investigation of ADAM feedstock and its rheological properties, a base for further development of new feedstocks intended for AM has been made.
3) The study addresses the issues connected to the merging of two progressive processing routes. The literature survey included has shown that there is so far no study comparing AM and PIM techniques systematically on the fixed part shape and dimensions using advanced statistical tools to derive the similarity of the investigated processing routes [14].

BIBLIOGRAPHY

[1] CHEN, Z., Z. Li, J. Li, et al. 3D printing of ceramics: A review. *Journal of the European Ceramic Society*. 2019, **39**(4), 661-687. doi:10.1016/j.jeurceramsoc.2018.11.013

[2] ORRÙ, R., R. LICHERI, A. M. LOCCI, A. CINCOTTI and G. CAO. Consolidation/synthesis of materials by electric current activated/assisted sintering. *Materials Science and Engineering: R: Reports*. 2009, **63**(4-6), 127-287. doi:10.1016/j.mser.2008.09.003

[3] BANDYOPADHYAY, A. and B. SUSMITA. *Additive Manufacturing*. Boca Raton: CRC Press, 2015. ISBN 9781498766708

[4] BENGISU, M. *Engineering ceramics*. New York: Springer, 2001. ISBN 3540676872

[5] SANETRNIK, D., B. HAUSNEROVA and V. PATA. Online Rheometry Investigation of Flow/Slip Behavior of Powder Injection Molding Feedstocks. *Polymers*. 2019, **11**(3). doi:10.3390/polym11030432

[6] HAUSNEROVA, B., B. N. MUKUND and D. SANETRNIK. Rheological properties of gas and water atomized 17-4PH stainless steel MIM feedstocks: Effect of powder shape and size. *Powder Technology*. 2017, **312**, 152-158. doi:10.1016/j.powtec.2017.02.023

[7] SANETRNIK, D., B. HAUSNEROVA, M. NOVAK and B. N. MUKUND. Effect of Particle Size and Shape on Wall Slip of Highly Filled Powder Feedstocks for Material Extrusion and Powder Injection Molding. *3D Printing and Additive Manufacturing*. 2023, **10**(2), 236-244. doi:10.1089/3dp.2021.0157

[8] BLEYAN, D. *Binder system for powder injection moulding: Polymerní pojiva pro vstřikování práškových materiálů*. Zlín, 2015. English Doctoral Thesis. Tomas Bata University in Zlín, Faculty of Technology, Department of Production Engineering. Supervisor Hausnerová, B. http://hdl.handle.net/10563/36781

[9] HAUSNEROVA, B., I. KURITKA and D. BLEYAN. Polyolefin Backbone Substitution in Binders for Low Temperature Powder Injection Moulding Feedstocks. *Molecules*. 2014, **19**(3), 2748-2760. doi:10.3390/molecules19032748

[10] MUKUND, B. N. and B. HAUSNEROVA. Variation in particle size fraction to optimize metal injection molding of water atomized 17–4PH stainless steel feedstocks. *Powder Technology*. 2020, **368**, 130-136. doi:10.1016/j.powtec.2020.04.058

[11] MUKUND, B. N., B. HAUSNEROVA and T. S. SHIVASHANKAR. Development of 17-4PH stainless steel bimodal powder injection molding

feedstock with the help of interparticle spacing/lubricating liquid concept. *Powder Technology*. 2015, **283**, 24-31. doi:10.1016/j.powtec.2015.05.013

[12] BLEYAN, D., P. SVOBODA and B. HAUSNEROVA. Specific interactions of low molecular weight analogues of carnauba wax and polyethylene glycol binders of ceramic injection moulding feedstocks. *Ceramics International*. 2015, **41**(3), 3975-3982. doi:10.1016/j.ceramint.2014.11.082

[13] HAUSNEROVA, B. and M. NOVAK. Environmentally Efficient 316L Stainless Steel Feedstocks for Powder Injection Molding. *Polymers*. 2020, **12**(6). doi:10.3390/polym12061296

[14] NOVAK, M., B. HAUSNEROVA, V. PATA and D. SANETRNIK. On the Possibilities of Merging Additive Manufacturing and Powder Injection Molding in the Production of Metal Parts. *Rapid Prototyping Journal* (Accepted). 2024.

[15] GERMAN, R. M. *Powder injection molding*. Princeton (NJ): Metal Powder Industries Federation, 1990. ISBN 9780918404954

[16] HAUSNEROVA, B., D. SANETRNIK and P. PONIZIL. Surface structure analysis of injection molded highly filled polymer melts. *Polymer Composites*. 2013, **34**(9), 1553-1558. doi:10.1002/pc.22572

[17] GERMAN, R. M. and A. BOSE. *Injection Molding of Metals and Ceramics*. Princeton (NJ): Metal Powder Industry Federation, 1996. ISBN 978-1878954619

[18] HAINES, P. J. Thermogravimetry. In: HAINES, P. J. *Thermal Methods of Analysis*. Dordrecht: Springer Netherlands, 1995, pp. 22-62. doi:10.1007/978-94-011-1324-3_2

[19] DIHORU, L. V., L. N. SMITH, R. ORBAN and R. M. GERMAN. Experimental Study and Neural Network Modeling of the Stability of Powder Injection Molding Feedstocks. *Materials and Manufacturing Processes*. 2000, **15**(3), 419-438. doi:10.1080/10426910008912997

[20] HAUSNEROVÁ, B. *Rheological approaches to powder injection moulding optimization: Reologický přístup k optimalizaci procesu vstřikování práškových směsí*. Zlín: Tomas Bata University in Zlín, 2011. Qualifying Lecture for Professorship. ISBN 9788073189969

[21] GREENE, C. D. and D. F. HEANEY. The PVT effect on the final sintered dimensions of powder injection molded components. *Materials & Design*. 2007, **28**(1), 95-100. doi:10.1016/j.matdes.2005.05.023

[22] HAUSNEROVA, B., L. CUCOVA and A. SORRENTINO. Effect of carbide powder characteristics on the PVT behavior of powder injection

molding compounds. *Powder Technology*. 2013, **237**, 627-633. doi:10.1016/j.powtec.2013.01.067

[23] HNATKOVA, E., B. HAUSNEROVA, A. HALES, L. JIRANEK, F. DERGUTI and I. TODD. Processing of MIM feedstocks based on Inconel 718 powder and partially water-soluble binder varying in PEG molecular weight. *Powder Technology*. 2017, **322**, 439-446. doi:10.1016/j.powtec.2017.09.029

[24] CARREAU, P. J., D. C. R. D. KEE and R. P. CHHABRA. *Rheology of Polymeric Systems: Principles and Applications*. Cincinnati (OH): Hanser Pub, 1997. ISBN 978-1569902189

[25] LAPOINTE, F., S. TURENNE and B. JULIEN. Low viscosity feedstocks for powder injection moulding. *Powder Metallurgy*. 2013, **52**(4), 338-344. doi:10.1179/003258909X12518163544239

[26] CROSS, M. M. Rheology of non-Newtonian fluids: A new flow equation for pseudoplastic systems. *Journal of Colloid Science*. 1965, **20**(5), 417-437. doi:10.1016/0095-8522(65)90022-X

[27] CARREAU, P. J. Rheological Equations from Molecular Network Theories. *Transactions of the Society of Rheology*. 1972, **16**(1), 99-127. doi:10.1122/1.549276

[28] VALENTE, E. H., V. K. NADIMPALLI, S. A. ANDERSEN, D. B. PEDERSEN, T. L. CHRISTIANSEN and M. A. J. SOMERS. Influence of atmosphere on microstructure and nitrogen content in AISI 316L fabricated by laser-based powder bed fusion. In: *Proceedings of the 19th International Conference and Exhibition (EUSPEN 2019)*. Cranfield (Bedfordshire): The European Society for Precision Engineering and Nanotechnology, 2019, pp. 244-247. ISBN 978-099577514-5

[29] LUO, J., X. JIA, R. GU, P. ZHOU, Y. HUANG, J. SUN and M. YAN. 316L Stainless Steel Manufactured by Selective Laser Melting and Its Biocompatibility with or without Hydroxyapatite Coating. *Metals*. 2018, **8**(7). doi:10.3390/met8070548

[30] RAZA, M. R., F. AHMAD, N. MUHAMAD, A. B. SULONG, M.A. OMAR, M. N. AKHTAR and M. ASLAM. Effects of solid loading and cooling rate on the mechanical properties and corrosion behavior of powder injection molded 316 L stainless steel. *Powder Technology*. 2016, **289**, 135-142. doi:10.1016/j.powtec.2015.11.063

[31] EBEL, T. PMTi2019: International conference on the PM and AM of titanium highlights a bright future for sinter-based technologies. *Powder Injection Moulding International*. 2019, **13**(4), 61–74.

[32] KUKLA, C., J. GONZALEZ-GUTIERREZ, S. CANO-CANO, S. HAMPEL, C. BURKHARDT, T. MORITZ and C. HOLZER. FUSED

FILAMENT FABRICATION (FFF) OF PIM FEEDSTOCKS. In: *Actas del VI Congreso Nacional de Pulvimetalurgia y I Congreso Iberoamericano de Pulvimetalurgia*. Ciudad Real, 2017, pp. 1-6.

[33] GONG, H., D. SNELLING, K. KARDEL and A. CARRANO. Comparison of Stainless Steel 316L Parts Made by FDM- and SLM-Based Additive Manufacturing Processes. *JOM*. 2019, **71**(3), 880-885. doi:10.1007/s11837-018-3207-3

[34] GALATI, M. and P. MINETOLA. Analysis of Density, Roughness, and Accuracy of the Atomic Diffusion Additive Manufacturing (ADAM) Process for Metal Parts. *Materials*. 2019, **12**(24). doi:10.3390/ma12244122

[35] BLEYAN, D., B. HAUSNEROVA and P. SVOBODA. The development of powder injection moulding binders: A quantification of individual components' interactions. *Powder Technology*. 2015, **286**, 84-89. doi:10.1016/j.powtec.2015.07.046

[36] HAUSNEROVA, B. Powder Injection Moulding - An Alternative Processing Method for Automotive Items. In: CHIABERGE, M, ed. *New Trends and Developments in Automotive System Engineering*. InTech, 2011, Ch. 7. doi:10.5772/13358

[37] HAUSNEROVA, B., L. MARCANIKOVA, P. FILIP and P. SAHA. Optimization of powder injection molding of feedstock based on aluminum oxide and multicomponent water-soluble polymer binder. *Polymer Engineering & Science*. 2011, **51**(7), 1376-1382. doi:10.1002/pen.21928

[38] RAZA, M. R., F. AHMAD, N. MUHAMAD, A. B. SULONG, M. A. OMAR, M. N. AKHTAR, M. ASLAM and I. SHERAZI. Effects of Debinding and Sintering Atmosphere on Properties and Corrosion Resistance of Powder Injection Molded 316 L - Stainless Steel. *Sains Malaysiana*. 2017, **46**(02), 285-293. doi:10.17576/jsm-2017-4602-13

[39] OMAR, M. A. and I. SUBUKI. Sintering Characteristics of Injection Moulded 316L Component Using Palm-Based Biopolymer Binder. In: SHATOKHA, V., ed. *Sintering - Methods and Products*. London: InTech, 2012, pp. 127-146. doi:10.5772/32737

[40] HWANG, I.-S., T.-Y SO, D.-H LEE and C.-S. SHIN. Characterization of Mechanical Properties and Grain Size of Stainless Steel 316L via Metal Powder Injection Molding. *Materials*. 2023, **16**(6), 2144. doi:10.3390/ma16062144

[41] GERMAN, R. M. *Metal Injection Molding: A Comprehensive MIM Design Guide*. Princeton (NJ): Metal Powder Industry Federation, 2011. ISBN 978-0981949666

[42] HNATKOVA, E., B. HAUSNEROVA and P. FILIP. Evaluation of powder loading and flow properties of Al_2O_3 ceramic injection molding feedstocks treated with stearic acid. *Ceramics International*. 2019, **45**(16), 20084-20090. doi:10.1016/j.ceramint.2019.06.273

[43] SOTOMAYOR, M. E., A. VÁREZ and B. LEVENFELD. Influence of powder particle size distribution on rheological properties of 316L powder injection moulding feedstocks. *Powder Technology*. 2010, **200**(1-2), 30-36. doi:10.1016/j.powtec.2010.02.003

[44] AGGARWAL, G., S.-J. PARK, I. SMID and R. M. GERMAN. Master Decomposition Curve for Binders Used in Powder Injection Molding. *Metallurgical and Materials Transactions A*. 2007, **38**(3), 606-614. doi:10.1007/s11661-007-9102-0

[45] LIN, D., D. SANETRNIK, H. CHO, et al. Rheological and thermal debinding properties of blended elemental Ti-6Al-4V powder injection molding feedstock. *Powder Technology*. 2017, **311**, 357-363. doi:10.1016/j.powtec.2016.12.071

[46] HAUSNEROVÁ, B., D. SANÉTRNÍK and V. PATA. Surface Properties of Powder Injection Moulded Parts Related to Processing Conditions. *Manufacturing Technology*. 2018, **18**(6), 895-899. doi:10.21062/ujep/197.2018/a/1213-2489/mt/18/6/895

[47] HAUF, G. and M. HÜTTER. PolyMIM® 316L, MSDS. *Version 01/09.2008*.

LIST OF SYMBOLS AND ABBREVIATIONS

Symbols

d_r Relative density of the sintered sample
D_{50} Diameter under which is 50 % of particles
D_{90} Diameter under which is 90 % of particles
Da Dalton
Ra Arithmetic mean deviation from the centerline of the profile
Rz Profile maximum height
RSm Profile average distance of the microscopic unevenness
V_S Volume of fully dense 17-4PH steel
$V_{Sint.}$ Volume of the sintered sample
V_0 Volume of the green sample
$\dot{\gamma}$ Shear rate
$\dot{\gamma}_a$ Apparent shear rate
η Material/compound viscosity
$\eta(\dot{\gamma})$ Shear rate-dependent viscosity
η_0 Zero-shear viscosity
η_a Apparent viscosity
η_b Viscosity of the pure binder
η_r Relative viscosity
τ_a Apparent shear stress

Abbreviations

ADAM Atomic diffusion additive manufacturing
AM Additive manufacturing
AW Acrawax C
BSD Backscattered electron detector
BSE Backscattered electrons
CA Cluster analysis
CW Carnauba wax
DMLS Direct metal laser sintering
$DMLS_{Blasted}$ DMLS samples with surface treatment
DSC Differential scanning calorimetry
EDX Energy-dispersive X-ray spectroscopy
FDM Fused deposition modeling
HT Heat treatment
MatEx Material extrusion
PCA Principal component analysis
PEG Polyethylene glycol
PIM Powder injection molding
PIM_{DMLS} PIM samples with DMLS powder
PIM_{PIM} PIM samples with PIM powder
PLA Polylactic acid
PW Paraffin wax
SA Stearic acid
SEM Scanning electron microscopy
SLM Selective laser melting
RPM Rotations per minute
TGA Thermogravimetric analysis
UTS Ultimate tensile strength
vol% Volume percentage
wt% Weight percentage
YS Yield strength

LIST OF FIGURES

Figure 1 Flow instabilities during rheological measurements of CW-based feedstock at 70 °C 11

Figure 2 Thermogravimetric analysis of AW-based feedstock with 316L powder after water debinding [13] 13

Figure 3 Microstructure of 316L steel sintered at: (a) 5 °C/min; (b) 15 °C/min [13] 15

Figure 4 Rheological measurements of utilized feedstocks (modified from [14]) 16

Figure 5 3D surface maps of: a) PIM_{PIM}; b) DMLS; c) ADAM [14] 20

LIST OF TABLES

Table 1 Setup of conditions for injection molding of Acrawax (AW) feedstock 11

Table 2 Mechanical properties of sintered 316L samples (modified from [13]) 14

Table 3 Mechanical properties of sintered samples made from 17-4PH steel (modified from [14]) 17

Table 4 EDX analysis of burned and unburnt samples of 17-4PH steel feedstock debound in a nitrogen atmosphere 18

Table 5 Surface parameters of DMLS, ADAM, and PIM samples [14] 19

CURRICULUM VITAE

Personal information

Martin Novák
7. 7. 1993
Drnovice 13
Drnovice 763 25, Czech Republic
m8_novak@utb.cz
+420 737 083 235

Education

2012 – 2015	Bc. - Tomas Bata University in Zlín, Faculty of Technology Bachelor's degree study program – Chemistry and Materials Technology (*B2808*) Study plan – Materials Engineering.
2015 – 2017	Ing. - Tomas Bata University in Zlín, Faculty of Technology Master study program – Chemistry and Materials Technology Study course – Materials Engineering.
2017 –	Ph.D. - Tomas Bata University in Zlín, Faculty of Technology Doctoral study program – Process Engineering Study course – Tools and Processes.

Personal skills

Mother tongue(s)	Czech
Other languages	English – B2-C1 German – A2
Driver's license	B
Digital skills	Microsoft Office™ Tools Graphics programs (Gimp) Data processing software (Minitab, Origin) FEA software (Samcef)

Training abroad:

1. Austria, EPMA Powder Metallurgy Summer School 2018, TECHNISCHE UNIVERSITÄT WIEN (1/7/2018 – 6/7/2018)
2. Poland, CEEPUS, POLITECHNIKA KRAKOWSKA - Krakow (31/3/2019 – 1/5/2019)

Projects:

1. OPPIK - CZ.01.1.02/0.0/0.0/20_324/0023586 - assistant of the knowledge transfer
2. CORNET - CZ.01.1.02/0.0/0.0/15_007/0001161: SmartNFR – performed a series of measurements for this project

LIST OF PUBLICATIONS AND PRESENTATIONS

Publications in Web of Science:

1. SANÉTRNÍK, Daniel, HAUSNEROVÁ, Berenika, **NOVÁK, Martin**, BHIMASENA RAO NAGARAJ, Mukunda. Effect of particle size and shape on wall slip of highly filled powder feedstocks for material extrusion and powder injection molding. *3D Printing and Additive Manufacturing*, 2022. ISSN 2329-7662. doi:10.1089/3dp.2021.0157
2. HAUSNEROVÁ, Berenika, **NOVÁK, Martin**. Environmentally efficient 316L stainless steel feedstocks for powder injection molding. *Polymers*, 2020, 12(6). ISSN 2073-4360. doi: 10.3390/polym12061296
3. KUBIŠOVÁ, Milena, **NOVÁK, Martin**, KOUTŇÁK, Rostislav, VRBOVÁ, Hana, ŽALUDEK, Milan, KNEDLOVÁ, Jana. Metrological Comparison between Heterogeneous Surfaces and their Imprints. *Manufacturing Technology*, 2022, 22(4), 429–435. doi:10.21062/mft.2022.046
4. VRBOVÁ, Hana, KUBIŠOVÁ, Milena, MĚŘÍNSKÁ, Dagmar, **NOVÁK, Martin**, PATA, Vladimir, KNEDLOVÁ, Jana, SEDLAČÍK, Michal, ŠUBA, Oldřich. The Implementation of Neural Networks for Polymer Mold Surface Evaluation. *Micromachines*. 2024, 15(1). ISSN 2072-666X. doi:10.3390/mi15010102
5. **NOVAK, Martin**, HAUSNEROVA, Berenika, PATA, Vladimir, SANETRNIK, Daniel. On the Possibilities of Merging Additive Manufacturing and Powder Injection Molding in the Production of Metal Parts, *Rapid Prototyping Journal* (Accepted). 2024.

Presentations and conferences:

6. KUBIŠOVÁ, Milena, **NOVÁK, Martin**, KOUTŇÁK, Rostislav, VRBOVÁ, Hana, ŽALUDEK, Milan. Metrologické srovnání heterogenních povrchů a jejich otisků. *6. mezinárodní konference Mikroskopie a nedestruktivní zkoušení materiálů, Hrubá Skála – Turnov, October 19-22, 2021, Czech Republic,* 2021.
7. MARCANÍK, Miroslav, KUBIŠOVÁ, Milena, PATA, Vladimír, **NOVÁK, Martin**, VRBOVÁ, Hana. Metrologické hodnocení heterogenních povrchů získané technologií řezání vodním paprskem pomocí prvků umělé inteligence. *6. mezinárodní konference Mikroskopie a nedestruktivní zkoušení materiálů, Hrubá Skála – Turnov, October 19-22, 2021, Czech Republic,* 2021.
8. SANÉTRNÍK, Daniel, HAUSNEROVÁ, Berenika, **NOVÁK, Martin**, BHIMASENA RAO NAGARAJ, Mukunda. Effect of Particle Size and Shape on Wall Slip of Highly Filled Powder Feedstocks for Powder Injection Molding. *Book of Abstract - 6TH International Conference on Competitive*

Materials and Technology Processes in Miskolc-Lillafüred, October 4-8, 2021, Hungary, 2021.

9. **NOVÁK, Martin**, ŠKROBÁK, Adam, HAUSNEROVÁ, Berenika, PATA, Vladimír, JANOVSKÝ, Petr, PTOŠKOVÁ, Barbora. A Practical Approach to Cleaning Molds from Rubber Residues. *2022 26th International Conference on Circuits, Systems, Communications and Computers, Chania, July 19-22, 2022*, *Greece*, 2022.
10. **NOVÁK, Martin**, HAUSNEROVÁ, Berenika. Environmentally Benign Binder Systems for MIM - optimization of molding conditions. *Development in Machining Technology DiM'2019 in Cracow, April 25 – 26th, 2019, Poland,* 2019

Optimalizace zpracování kovových prášků vstřikováním

Powder Injection Molding: Feedstock Tailoring and Process Optimization

Doctoral Thesis Summary

Published by: Tomas Bata University in Zlín,

nám. T. G. Masaryka 5555, 760 01 Zlín.

Edition: published electronically

Typesetting by: Ing. Martin Novák, Ph.D.

This publication has not undergone any proofreading or editorial review.

Publication year: 2024

First Edition

ISBN 978-80-7678-244-0